

Wastewater Treatment Process Improvement using Fate Modeling of Xenobiotic Organic Compounds

Rosita Ghalajkhani¹, Kelly Weeks², and Mahdi Safa¹

¹University of Houston

²Lamar University

November 23, 2022

Abstract

The presence of Xenobiotic Organic Compounds (XOCs) in municipal wastewater treatment plants' effluent raises a global concern due to the easy consumption of these micropollutants by organisms. The fate of XOCs removal mechanisms of these compounds remains a challenge in recent scientific research. This study aimed to create an uncalibrated mathematical fate model within the professional wastewater modeling simulation software in a first step that was able to address the fate of Sulfamethoxazole (SMX), its metabolite, and Nonylphenol ethoxylates (NPEOs) along with conventional compounds during an activated sludge process. For the calibration process as a next step, two different case studies were created with assigning related removal mechanisms to each group of compounds. In the calibration process, model parameters are tuned such that the model can best simulate the experimental data using optimization methods. The validation results showed that the proposed model successfully simulates the removal of XOCs. Results of sensitivity analysis showed that the fate model is more sensitive to biodegradation rate constant than Solid Retention Time (SRT).

1
2 **Wastewater Treatment Process Improvement using Fate Modeling of Xenobiotic**
3 **Organic Compounds**

4 **R. Ghalajkhani¹, K. Weeks², and M. Safa³**

5 ¹ Research Assistant, Civil and Environmental Engineering, University of Houston, Katy
6 Academic Building, 22400 Grand Circle Blvd., Suite 307, Katy, Texas 77449.

7 ² Associate Professor of Management, College of Business, 4400 MLK Blvd., PO Box 10009,
8 Beaumont, Texas 77710.

9 ³ Senior Lecturer, Civil and Environmental Engineering, University of Houston, Katy Academic
10 Building, 22400 Grand Circle Blvd., Suite 307, Katy, Texas 77449.

11 Corresponding author: Mahdi Safa (msafa@uh.edu)

12 **Key Points:**

- 13 • The developed fate model can be used to optimize the removal process of Xenobiotic
14 Organic Compounds (XOCs)
- 15 • The removal efficiency of the SMX was found to be negative, because the conjugate was
16 converted to SMX during the biotransformation process
- 17 • Sensitivity analysis of three different cases showed that the fate model was more
18 sensitive to biodegradation rate than to sorption rate.
19

20 Abstract

21 The presence of Xenobiotic Organic Compounds (XOCs) in municipal wastewater treatment
22 plants' effluent raises a global concern due to the easy consumption of these micropollutants by
23 organisms. The fate of XOCs removal mechanisms of these compounds remains a challenge in
24 recent scientific research. This study aimed to create an uncalibrated mathematical fate model
25 within the professional wastewater modeling simulation software in a first step that was able to
26 address the fate of Sulfamethoxazole (SMX), its metabolite, and Nonylphenol ethoxylates
27 (NPEOs) along with conventional compounds during an activated sludge process. For the
28 calibration process as a next step, two different case studies were created with assigning related
29 removal mechanisms to each group of compounds. In the calibration process, model parameters
30 are tuned such that the model can best simulate the experimental data using optimization
31 methods. The validation results showed that the proposed model successfully simulates the
32 removal of XOCs. Results of sensitivity analysis showed that the fate model is more sensitive to
33 biodegradation rate constant than Solid Retention Time (SRT).

34 1 Introduction

35 Organic micropollutants have attracted significant concern from the scientific community
36 because of their environmental fate and hazardous/ toxicological properties. These hazardous
37 pollutants, which threaten human life and the environment, typically should have low
38 concentrations of which range from ng/L to a few hundred µg/L in wastewater effluents. Many
39 recent studies show the conventional wastewater treatment plants (WWTPs) are not able to
40 remove these emerging compounds properly (Rathi, et al., 2021; Wang, et al., 2021; Jari, et al.,
41 2022; Xiang, et al., 2022; Zhou, et al., 2022). Hence this study aims to address removal
42 mechanisms of these compounds precisely and efficiently which in turn leads to improving the
43 design and operational condition of WWTPs. With proper formulation of such innovative
44 methods, the presence of hazardous materials in the environment can be assured within proper
45 ranges. Thus, adverse effect on human/ aquatic life will be reduced significantly leading to a
46 sustainable water cycle in an effort to promote means of human societies to reuse water.

47 Municipal wastewater contains a complex mixture of XOCs originating from personal
48 care products, pharmaceuticals, secreted hormones, household, and industrial chemicals. These
49 anthropogenic XOCs are of concern due to the increasing number of reports of reproductive
50 disorders in aquatic wildlife residing below wastewater outfalls (Al Qarni et al., 2016; Maiti et
51 al., 2016; Martin-Pascual et al., 2020; Quintelas et al., 2020). Several recent studies have
52 estimated that wastewater could contain many types of XOCs. Particular XOCs, that are known
53 to cause toxic effects in different recipients and species, are frequently reported in WWTP
54 effluents in potentially toxic concentrations (Hamza et al., 2016; Wilson & Ashraf, 2018; Çeçen
55 & Gül, 2020; Choudhary & Philip, 2021). In addition, these chemicals may cause long-term
56 changes in aquatic ecosystems because of intrinsic properties such as high polarity and
57 persistence (Baalbaki et al., 2017; Cheng et al., 2017). Feminization of male fish in different
58 species is a well-known effect observed in recipients loaded with treated wastewater.
59 Experiments with caged fish have confirmed that wastewater containing Endocrine Disrupting
60 Compounds (EDC) can cause feminization. XOCs in freshwater has been observed and found
61 to constitute a serious risk to human health and aquatic life (Contreras et al., 2019; Hai et al.,
62 2016; Martin-Pascual et al., 2020; Wilson & Ashraf, 2018). Wastewater treatment plants
63 (WWTPs) remove XOCs from the water mainly by sorption, biological and/or chemical

64 degradation, volatilization, and/or stripping. Conventional wastewater treatment is not directly
65 designed for removing XOCs but nonetheless reduces the concentration of several key XOCs
66 (Compagni et al., 2020; Contreras et al., 2019; van Bergen et al., 2020). Several studies have
67 identified the biodegradation and sorption of XOCs as a vital elimination process in WWTPs
68 (Baalbaki et al., 2017; Plósz & Ramin, 2019; van Bergen et al., 2020). However, the ability to
69 utilize and control the parameters and processes governing the biodegradation of XOCs in
70 activated sludge systems remains a challenge. Therefore, models developed and calibrated from
71 experiments, with carefully selected model pollutants, should be constructed to support scientists
72 efforts to discover and realize optimal treatment levels (Hatoum et al., 2019; Plósz & Ramin,
73 2019; Quintelas et al., 2020; Compagni et al., 2020).

74 Not all of the aforementioned processes are conducive for removing XOCs. For this
75 reason, these compounds should be categorized regarding related mechanisms. For example,
76 Nonylphenol Ethoxylates (NPEOs) are a class of compounds that are transformed by the abiotic
77 cleavage process. In aerobic systems, the major pathway of biodegradation for NPEOs is
78 stepwise oxidation and cleavage of the polyoxyethylene chain either by hydrolysis or an
79 oxidative hydrolytic mechanism before biodegradation of this compound. Hence, these
80 compounds are transformed by the abiotic cleavage process along with biodegradation and biotic
81 hydrolysis (Karahan et al., 2010; Zonja et al., 2015; Aymerich et al., 2016). Another important
82 class of compounds, used extensively in both human and veterinary medicine, is antibiotic
83 sulfamethoxazole (SMX). The specific removal mechanisms for these compounds are aerobic
84 and anoxic parent compound formation, co-metabolism, competitive inhibition along with
85 normal aerobic and anoxic biodegradation and aerobic/anoxic sorption (Achermann et al., 2018;
86 Plósz & Ramin, 2019; Brown et al., 2020; Çeçen & Gül, 2020; Compagni et al., 2020). In this
87 work, the first step was recognition of removal mechanisms and compound categorization, which
88 led to two influential case studies. The second step is fate modeling. In this step, the most recent
89 models are investigated and compared. Most of the existing models describe the fate of XOC
90 without including more complex mechanisms such as parent compound transformation, co-
91 metabolism, etc. Only a few models have considered biodegradation in aerobic and anoxic
92 conditions (Plósz et al., 2009; Suarez et al., 2010; Cheng et al., 2017; NELSON et al., 2018;
93 Quintelas et al., 2020). In most fate models, the volatile fraction of total biomass has been
94 employed in the biokinetic rate equations. This study's model will develop and separate a
95 heterotrophic biomass, which will describe its role in the fate of XOCs more precisely than
96 current models. Activated sludge model 1, ASM1, (by International Water Association (IWA))
97 was developed for the design and operation of biological wastewater treatment plants and
98 removal of conventional contaminants; however, these models were not designed to predict the
99 fate and transport of XOCs.

100 The objective of this work was to develop and critically evaluate an enhanced fate model
101 for XOCs in wastewater treatment plants. Mechanisms that are responsible for the removal of
102 XOCs in wastewater treatment were identified and integrated with an ASM1 model to create an
103 uncalibrated fate model. Activated sludge models (ASM) can differentiate between viable and
104 non-viable biomass, so it was expected that ASM-based integrated fate models should be able to
105 provide more accurate predictions of XOC fate over a range of operating conditions. The newly
106 created fate model will initially be incorporated into the GPS-X process simulator to create an
107 uncalibrated fate model. Since only a small group of mechanisms is responsible for the removal
108 of each compound, for the next step, mechanisms are categorized in two different case studies.
109 Each case study will be individually calibrated and validated using corresponding data from the

110 literature. The combined enhanced model will be critically evaluated by conducting a sensitivity
111 analysis that will evaluate the impact of operational and modeling parameters, such as Solid
112 Retention Time (SRT), and biodegradation and partitioning coefficients, on the contaminant fate
113 model (van Bergen et al., 2020; Wang et al., 2020). The proceeding section discusses the fate
114 model structure which describes schematic modeling processes, case study descriptions
115 including assigned specific removal mechanisms to each group of compounds, and model
116 calibration processes that use optimization methods. Model parameters were 'tuned' such that the
117 model could best follow the experimental data. Ultimately, results and analysis are provided to
118 enhance modeling outputs and results discussions.

119 **2 Fate Model Structure**

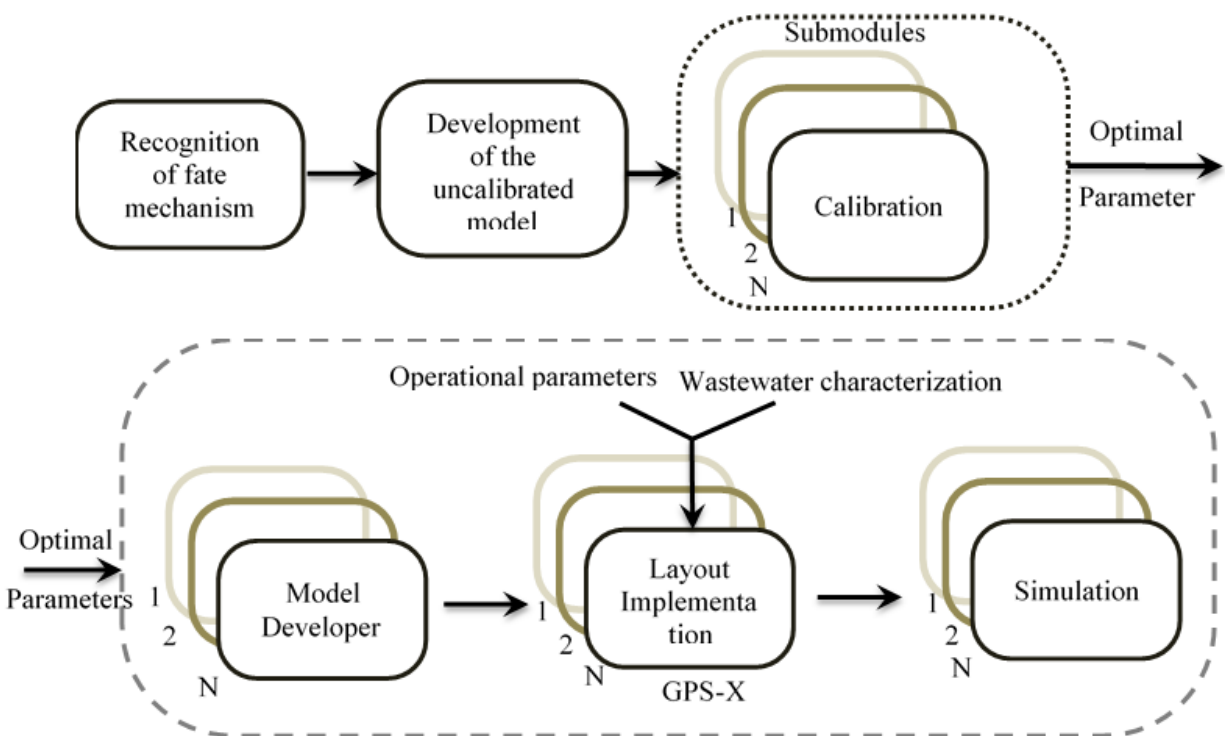
120 The International Association on Water Pollution Research and Control (IAWPRC) task
121 group realized that, due to the long solids retention times and low growth rates of bacteria, actual
122 effluent substrate concentrations between different activated sludge treatment plants did not vary
123 greatly. What significantly differed was the levels of MLSS and electron acceptor (oxygen or
124 nitrate). Thus the focus of the Activated Sludge Model No.1 (ASM1) is the prediction of the
125 solids generation and electron acceptor consumption (Plósz et al., 2009; Pomiès et al., 2013).
126 This works model is employed to predict the viable biomass in the activated sludge process
127 (heterotroph biomass). The main reason to use the ASM 1 model is the ability of this particular
128 model to simulate biomass growth and differentiate between viable and non-viable biomass
129 under aerobic and anoxic condition in WWTP studies, which is vital to accurate prediction of
130 XOCs fate in WWTPs. It should be noted that instead of using X_{ss} to describe the biomass
131 concentration (as is traditionally employed in fate modeling) x_{bh} was employed to take
132 advantage of the integration of the fate model within the ASM based model.

133 The software GPS-X was used to carry out simulation results. This software is a multi-
134 purpose modeling tool that can be employed for the simulation of municipal and industrial
135 wastewater treatment plants. This software package provides conventional models such as ASM
136 1 as built-in libraries that can be used as a basis on which new models can be created. Within the
137 GPS-X software, the Mantis model is used which is identical, with minor modifications, to ASM
138 1. A library within GPS-X details a list of wastewater process models using a set of basic
139 wastewater components or state variables. The term state variable refers to the basic variables
140 that are continuously integrated over time. The composite variables are those variables that are
141 calculated from (or composed of) the state variables. The relationships between the state and
142 composite variables are calculated at every connection point of the plant layout. For this
143 research, the Industrial Pollutant Variables Library (CNIPLIB) was used. This library includes
144 forty-six state variables: sixteen are predefined and thirty are user defined (15 soluble, 15
145 particulate). These state variables are used for fate model variables. For example, SMX in the
146 solid phase, describes X_{za} while the soluble species describes S_{zf} .

147 The integrated fate model employs an ASM-based (Mantis) model for prediction of
148 viable biomass that is subsequently responsible for removal and transformation of trace
149 compounds. Hence, the model is able to be employed for predicting the removal of conventional
150 and trace compounds simultaneously. The "model developer", which is a software tool
151 developed by Hydromantis was used to generate the ASM based fate model. To create the new
152 model in GPS-X, the model developer included the Mantis model matrix as the basis and the
153 CNIPLIB library was used. CNIPLIB was selected as it has the capacity to employ a number of

154 pre-defined states for industrial customized components that in this article consisted of the target
 155 XOC's. The model developer contains several spreadsheets with the first spreadsheet containing
 156 the fate model matrix. The second sheet includes the composite variables vector for GPS-X. The
 157 third sheet contains the fate model parameters and coefficients, such as state variables, composite
 158 variables, and the stoichiometric and kinetic parameters, for both the conventional and the trace
 159 compounds. The last sheet contains the list of the GPS-X library state variables. The model
 160 developer converts the matrix components to a language that can be read by the GPS-X software.

161 Figure 1 depicts the workflow for the modeling process. Since specific groups of
 162 mechanisms were identified to be responsible for the removal of selected compounds, two
 163 different case studies were created for two different groups of compounds. Hence, two different
 164 submodels were created within the fate model. Each submodel was generated in the GPS-X
 165 software separately. To achieve this goal, compounds that were not included in a specific
 166 submodel, were omitted by inserting zero values in the corresponding rows and columns. For
 167 example, for Case Study 1, this was created for removal of SMX process rates and compounds
 168 that were not related to SMX fate were zeroed. The two different submodels were calibrated
 169 separately using relevant literature data for both the conventional and trace compounds, and the
 170 optimal parameters were obtained and inserted in the corresponding sheet of the model developer
 171 (third sheet). After this step, each submodel was generated in the GPS-X software by using the
 172 model developer tool, and the simulation results were reported.



173
 174

Figure 1. Schematic modeling process flow chart of this work

175 3 Case Studies Description

176 Since only selected mechanisms are responsible for the removal of a specific compound,
 177 two different case studies (two sub models) were developed for use in this study. Each case
 178 study addressed a specific group of compounds. First case study was created to address the

179 biodegradation and sorption of SMX along with biodegradation (conversion) of its metabolite to
 180 the parent compound (SMX). The removal mechanisms for these compounds are: aerobic and
 181 anoxic biodegradation, parent compound formation, co-metabolism and competitive inhibition
 182 and aerobic and anoxic sorption. In developing case study 1, all process rates and compound
 183 species that were not related to the SMX and its metabolite removal were omitted from the fate
 184 model matrix by inserting zeros in the relevant rows and columns. The submodel for this case
 185 was a Mantis based model that addressed the removal of SMX and its metabolite along with the
 186 conventional compounds. The Matrix for the SMX and its metabolite was presented in Table 1.

Table 1: process matrix of SMX and its metabolite

SMX and its metabolite components			Process rate	Process rate description
Szf	Szg	Xza		
-1	0	0	$k_{1BioOx} \cdot Szf \cdot \frac{(K_s \cdot \eta_{bio})}{(K_s \cdot \eta_{bio} + S_s)} \cdot \frac{S_o}{(K_o + S_o)} \cdot xbh$	Aerobic biotransformation of Szf
1	-1	0	$k_{1DecOx} \cdot Szg \cdot \frac{(K_s \cdot \eta_{DEC})}{(K_s \cdot \eta_{DEC} + S_s)} \cdot \frac{S_o}{(K_o + S_o)} \cdot xbh$	Aerobic parent compound transformation
-1	0	0	$k_{1BioAX} \cdot Szf \cdot \frac{(K_s \cdot \eta_{bio})}{(K_s \cdot \eta_{bio} + S_s)} \cdot \frac{S_o}{(K_o + S_o)} \cdot xbh$	Anoxic biotransformation of Szf
1	-1	0	$k_{1DecAX} \cdot Szg \cdot \frac{(K_s \cdot \eta_{DEC})}{(K_s \cdot \eta_{DEC} + S_s)} \cdot \frac{S_o}{(K_o + S_o)} \cdot xbh$	Anoxic parent compound transformation
1	0	-1	$K_{Des} \cdot Xza \cdot \frac{S_o}{(K_o + S_o)}$	Aerobic desorption of Szf
-1	0	1	$K_{Des} \cdot K_{1DOx} \cdot Szf \cdot \frac{S_o}{(K_o + S_o)} \cdot X_{ss}$ $K_{Des} \cdot K_{1DAx} \cdot Szf \cdot \frac{K_o}{(K_o + S_o)} \cdot X_{ss}$	Aerobic sorption of Szf
1	0	-1	$K_{Des} \cdot Xza \cdot \frac{K_o}{(K_o + S_o)}$	Anoxic desorption of Szf
-1	0	1	$K_{Des} \cdot K_{1DAx} \cdot Szf \cdot \frac{K_o}{(K_o + S_o)} \cdot X_{ss}$	Anoxic sorption of Szf

187 Two major mechanisms are responsible for removal of SMX: biodegradation and
 188 sorption. For fate modeling of this compound, the impact of aerobic and anoxic conditions was
 189 considered for both biodegradation and sorption mechanisms. The biodegradation of its
 190 metabolite (daughter compound, Szg) was also considered in this model. The metabolite that was
 191 present in the raw wastewater during the biodegradation process was converted to the parent
 192 compound (SMX). The expressions for the process rates of aerobic/anoxic biodegradation, and
 193 aerobic/anoxic parent and daughter compounds transformation contain modifying terms, (1) and
 194 (2) respectively that reduce the rates in the presence of readily biodegradable COD. The uptake

195 of readily biodegradable COD (S_s) has been reported to cause competitive inhibition of micro
 196 pollutant biotransformation processes (Plósz et al., 2009).

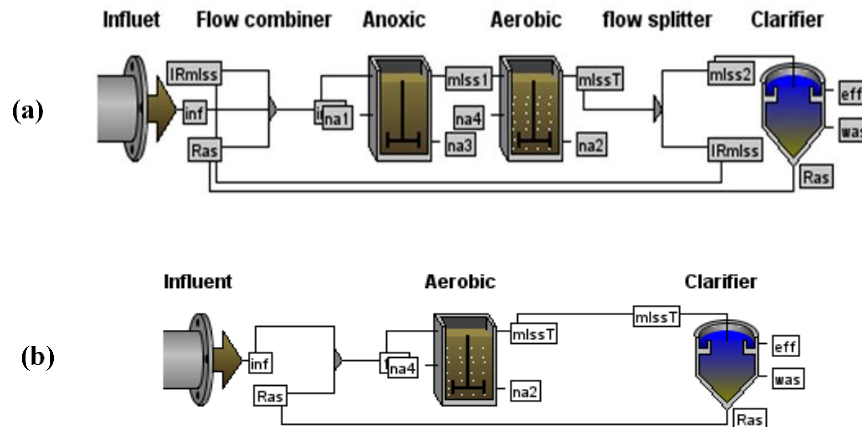
197

$$\frac{(K_s \cdot \eta_{bio})}{(K_s \cdot \eta_{bio} + S_s)} \quad (1)$$

$$\frac{(K_s \cdot \eta_{1DEC})}{(K_s \cdot \eta_{1DEC} + S_s)} \quad (2)$$

198 (Plósz et al., 2009) observed an increase in the concentration of SMX, through
 199 wastewater treatment with negative or low removal efficiencies observed for this compound.
 200 Therefore it was concluded that other mechanisms should be taken into account during the
 201 removal of this compound (Plósz et al., 2009; Sipma et al., 2010). It is possible for certain
 202 pharmaceuticals that the conjugated form may be present in the raw wastewater at concentrations
 203 greater than of the parent. Thus a mechanism referred to as parent compound transformation was
 204 added. Equations 10 and 12 describe the process rates for the aforementioned phenomenon.

205 The model in this case study was calibrated using the data provided in (Plósz et al.,
 206 2009). The plant configuration for this study is shown in Figure 2. Since aerobic and anoxic
 207 biodegradation were included as removal mechanisms for SMX and its metabolite removal,
 208 aerobic and anoxic compartments were employed in the activated sludge process plant. For the
 209 sensitivity analysis of this case against SRT, only aerobic parent compound transformation,
 210 aerobic biodegradation, and aerobic sorption-desorption were considered to simplify the data
 211 interpretation.



212

213 Figure 2. (a) Plant configuration for the removal of SMX; (b) Plant configuration for the
 214 removal of NPEOs

215 Second case study assessed the fate of nonylphenol ethoxylates (NPEOs) in an activated
 216 sludge process. The removal mechanisms for this compounds includes abiotic oxidative
 217 cleavage, biotic hydrolysis and aerobic biodegradation. A specific mechanism that has been
 218 reported to contribute to the removal of NPEO's is an abiotic oxidative cleavage process
 219 (Karahana et al., 2010). In this process, the NPEO's are converted to slowly biodegradable
 220 NPEOs, readily biodegradable NPEOs and non-biodegradable NPEOs. In addition, through a

221 hydrolysis process the slowly biodegradable portion of this compound is converted to the readily
 222 biodegradable form, and then this portion is biodegraded during the growth processes. This sub
 223 model was designed to predict the fate of NPEO's along with conventional compounds that was
 224 based on the Mantis model. The process rates are described in Table 2.

Table 2: process matrix of NPEO

NPEO Components				Process rate	Process rate Description
Sza	Szb	Szc	Szd		
$-(1-f_{\text{INPEO}})$	α	$1-\alpha$	f_{INPEO}	$K_{\text{OCL}} \cdot Sza$	Abiotic cleavage
0	1	-1	0	$k_{\text{hNPEO}} \cdot \left[\frac{(Szc / xbh)}{K_{\text{xNPEO}} + (Szc / xbh)} \right] \cdot xbh$	Hydrolysis of NPEO
0	-1	0	0	$K_{\text{bioNPEO}} \cdot Szb \cdot \frac{K_s}{(K_s + S_s)} \cdot \frac{S_o}{(K_{\text{oh}} + S_o)} \cdot xbh$	Growth on SS _{NPEO}

225 The structure of the expression for the hydrolysis rate of NEPO's is similar to that of
 226 entrapped organics in Mantis model. The biodegradation structure of the SSNPEO is similar to
 227 that employed for the biodegradation of SMX and included a modifying term for readily
 228 biodegradable substrate $[(K_s)/(K_s+S_s)]$ as the uptake of Ss can reduce the biodegradation of
 229 SSNPEO (Karahana et al., 2010). In this case study the model was calibrated using the
 230 experimental data provided in (Karahana et al., 2010). The plant configuration for this study is
 231 shown in Figure 2b. The WWTP physical and operational parameters are shown in Table 2.
 232 These parameters were also extracted from (Karahana et al., 2010).

233 In the calibration process, using optimization methods, model parameters can be 'tuned'
 234 such that the model can best follow the experimental data. A common error metric is Sum of
 235 Squared Errors (SSE) between the simulated results and measured data, optimal values of
 236 parameters of interest were found. Equation 1 shows the objective function for the calibration:

$$SSE = \sum_{i=1}^n SSE_i \quad \text{with} \quad SSE_i = \left(\frac{y_i^{\text{sim}} - y_i^{\text{exp}}}{y_i^{\text{exp}}} \right)^2 \quad (3)$$

237 Where y_i^{sim} and y_i^{exp} are the simulated and measured values of the response variable y
 238 (usually effluent substrate concentration), respectively. Index i refers to the ith data point where
 239 the total number of data points is n in the experimental process. Although using optimized
 240 parameter values, the model can best describe the system behaviour, in some cases, these
 241 parameter values are infeasible (Lindblom et al., 2009). Hence in the optimization problem,
 242 lower and upper bounds were added to the model parameters to avoid infeasible values for
 243 parameters. Therefore, the calibration process formulation was written as:

$$\begin{aligned} \min \quad & SSE(t, P) \\ \text{LB}_j \leq & P_j \leq \text{UB}_j \end{aligned} \quad (4)$$

244 Where SSE is a function of time and vector of parameters P, LB and UB are the lower
 245 bounds and upper bounds on the parameter, and index j refers to the jth parameter. In this study,
 246 minimum and maximum values that were obtained from literature were adopted as LB and UB.
 247 For each calibration, parameters were obtained by solving the optimization problem using the
 248 Genetic Algorithm (GA) in MATLAB. To ensure the optimality of the parameter values, GA
 249 was run for two times, and then the parameters corresponding to the least objective function were
 250 put into the Pattern Search function as a Direct Search (DS) routine until the change in the
 251 objective function and constraint violation values were less than 1E-6. At this point the resulting
 252 values were accepted to provide the global optimum. The uncertainties involved in the
 253 calibration process are computed by means of a numerical method explained in (Draper & Smith,
 254 1981). In a general case, the objective function J can be multi-objective, and defined as:

$$J = \sum_{i=1}^n J_i \quad \text{with} \quad J_i = \mu_1 \left(\frac{y_{i1}^{sim} - y_{i1}^{exp}}{y_{i1}^{exp}} \right)^2 + \mu_2 \left(\frac{y_{i2}^{sim} - y_{i2}^{exp}}{y_{i2}^{exp}} \right)^2 + \dots \quad (5)$$

255 Where μ_1, μ_2, \dots are the weights of different terms in the objective function and y_{ij} are the
 256 values of the multiple responses. Assuming a linear behavior for the response, this approach
 257 approximates the mean square error for each parameter from the sensitivity of the objective
 258 function to each parameter and a variance defined as follows:

$$\sigma^2 = \frac{\hat{J}}{n-p} \quad (6)$$

259 Where \hat{J} is the objective function value at the optimal point, n is the number of
 260 observations, and p is the number of calibration parameters. Additionally, the sensitivity can be
 261 approximated in discrete form as follows:

$$\frac{\partial J_i}{\partial P_j} \simeq \frac{J_i(\hat{P}_j + \Delta P_j) - J_i(\hat{P}_j)}{\Delta P_j} \quad (7)$$

262 where \hat{P}_j is the optimal estimate of parameter P, index i refers to the ith data point, index
 263 j refers to the jth parameter, $\hat{P}_j + \Delta P_j$ is the perturbed parameter, $J_i(\hat{P}_j + \Delta P_j)$ is the objective
 264 function at the perturbed parameter value, and $J_i(\hat{P}_j)$ is the objective function value at the optimal
 265 parameter estimate. Note that J_i is equal to the SSE_i in case the objective function is single
 266 objective, as defined in equation 1. Then the sensitivity matrix can be formed as follows:

$$S = \begin{bmatrix} S_{11} & S_{12} & \dots & S_{1p} \\ S_{21} & S_{22} & \dots & S_{2p} \\ \vdots & \vdots & S_{MN} & \vdots \\ S_{p1} & S_{p2} & \dots & S_{pp} \end{bmatrix} \quad (8)$$

267 The sensitivity matrix is a symmetric square matrix (pxp) that includes the sensitivity of
 268 the objective function with respect to all calibration parameters. Each component is defined as:

$$S_{MN} = \sum_{i=1}^n \frac{\partial J_i}{\partial P_M} \frac{\partial J_i}{\partial P_N} \quad \text{with } M, N \in \{1, 2, \dots, p\} \quad (9)$$

269 Then the 95% confidence interval for each parameter is acquired as:

$$\hat{P}_j \pm 1.96\sqrt{V_{jj}} \quad \text{with } V = \sigma^2 S^{-1} \quad (10)$$

270 Equation 10 calculates the interval for the *j*th estimated parameter with 95% confidence.
 271 By extracting data from the output of this calibration process, which was done for both
 272 conventional and trace compounds, the following results were found that are in the next section.

273 **4 Results and Analysis**

274 Fate modeling procedure in this work was done mainly by calibration and validation
 275 procedure, which required at least a primary and secondary experimental data set. Although
 276 measuring and obtaining these experimental data still remains a challenge especially for these
 277 micro pollutants, data for this work was extracted from proven scientific resources and fit
 278 correctly in the shape and operational condition of WWTPs.

279 The calibration of the model for case study 1 was performed for both conventional and
 280 fate model parameters. Since the estimation of biomass production is one of the key parameters
 281 for addressing the fate of trace compounds, matching of the biomass production in the steady
 282 state condition with the data set was employed for calibration. The experimental data presented
 283 in (Plósz et al., 2009) was used for the calibration of this model. The data set for the SMX was
 284 presented from continuous effluent flow of both the anoxic and aerobic reactor (Figure 3) in
 285 soluble form. Since the full data set was not available, the conventional parameters including
 286 total COD, inert inorganic suspended solids, particulate inert organic material, total suspended
 287 solids in the wastewater influent, plant configuration, and plant operational parameters, (SRT=16
 288 days and HRT=5.33 hr) were set to those described by (Plósz et al., 2009). For other ASM1
 289 parameters that were not reported in the related literature, the default values for municipal
 290 wastewater treatment plants were employed. By adjusting the inert organic suspended solids,
 291 influent VSS and the ratio of inert particulate COD to biodegradable COD in the wastewater
 292 influent by trial and error within the GPS-X software, and running simulations on the submodel
 293 of this case study, the biomass concentration in the bioreactor at steady state was matched with
 294 the corresponding experimental data presented in the literature. The relative error for this
 295 calibration was 0.5%. Active biomass is not measurable experimentally; thus, it is often
 296 assumed in fate models that the MLSS or MLVSS can represent the active biomass. However, in
 297 the new fate model that was developed in this research, the active heterotrophic biomass was
 298 used as the active fraction of the MLSS and was predicted by the conventional part of the model
 299 within GPS-X. Hence, the parameter values (*k_b*, *k_d*, etc) predicted in this research can be
 300 expected to be different from that reported in the literature. After conventional parameter
 301 calibration, according to the plant layout and submodel matrix, a corresponding set of differential
 302 equations were transferred to MATLAB where the fate model was calibrated with experimental
 303 data reported for the trace compound (SMX). To this goal, for each parameter of interest in the
 304 structure of the model matrix, the mean (μ) and standard deviation (σ) of the literature reported
 305 ranges were calculated. The mean and standard deviation were calculated over those reported in
 306 each reference, i.e., in most references, the reported values were in the form of uncertainty
 307 ranges ($\mu \pm \sigma$). Then lower and upper bounds for the calibration parameters were set to $\mu - \sigma$ and
 308 $\mu + \sigma$, respectively, see Table 3. For the anoxic bioreactor, as the work by (Plósz et al., 2009)

309 provided the only reported parameter values, the lower and upper bounds were set to 0.1 and 10
 310 times the reported. For this case, the following objective function was considered:

$$\begin{aligned}
 SSE = & 0.25 \sum_{i=1}^n \left(\frac{Szf_{i,aerobic}^{sim} - Szf_{i,aerobic}^{ref}}{\max(Szf_{aerobic}^{ref})} \right)^2 + 0.25 \sum_{i=1}^n \left(\frac{Szg_{i,aerobic}^{sim} - Szg_{i,aerobic}^{ref}}{\max(Szg_{aerobic}^{ref})} \right)^2 + \\
 & 0.25 \sum_{i=1}^n \left(\frac{Szf_{i,anoxic}^{sim} - Szf_{i,anoxic}^{ref}}{\max(Szf_{anoxic}^{ref})} \right)^2 + 0.25 \sum_{i=1}^n \left(\frac{Szg_{i,anoxic}^{sim} - Szg_{i,anoxic}^{ref}}{\max(Szg_{anoxic}^{ref})} \right)^2
 \end{aligned} \tag{11}$$

311 where index *i* refers to the *i*th data point, $Szf_{aerobic}^{sim}$ is the simulated value for Szf (effluent
 312 concentration of SMX), Szf_{anoxic}^{sim} is the simulated value for Szf (effluent of anoxic reactor),
 313 $Szf_{aerobic}^{ref}$ and Szf_{anoxic}^{ref} represent the experimental data for Szf in effluent of aeration and anoxic
 314 reactor, respectively from (Plósz et al., 2009), $Szg_{aerobic}^{sim}$ is the simulated Szg (the compound
 315 concentration biotransformed via the Szf in aerobic reactor effluent), Szg_{anoxic}^{sim} is the simulated
 316 Szg in effluent of anoxic reactor, and Szg_i^{ref} denotes the model results by (Plósz et al., 2009).
 317 Note that no experimental data was reported for Szg (Plósz et al., 2009). The objective function
 318 is written in a non-dimensionalized form to provide relatively similar effects of the two terms on
 319 the SSE; otherwise, the four terms could have such different values the optimizer would mostly
 320 reduce only the larger terms. A summary of the calibration results is presented in the following
 321 table:

Table 3: Calibration results for case study 1

Parameter	Lower Bound	Upper Bound	Optimal Value ± Standard Error
K_{1BioOx} (m ³ /gbiomass/d)	6.937E-4	1.904E-3	1.529E-3±3.7E-4
K_{1BioAx} (m ³ /gbiomass/d)	6.937E-4	1.904E-3	1.529E-3±3.7E-4
K_{1DecOx} (m ³ /gbiomass/d)	6.8E-4	6.8E-2	3.312E-2±6.3E-3
K_{1DecAx} (m ³ /gbiomass/d)	7.85E-4	7.85E-2	3.823E-2±5.8E-3
K_{1Dox} (m ³ /gbiomass)	5.110E-5	3.893E-4	2.914E-4±3.4E-5
K_{1DAx} (m ³ /gbiomass)	5.5E-5	5.5E-3	5.500E-4±4.1E-5
η_{bio}	1	3	2.886±0.46
η_{1Dec}	1	3	1.920±0.31

322 Following calibration, the fate model for case study 1 was validated with a different data
 323 than that used for calibration; therefore, in the validation phase, the experimental results of
 324 (Suarez et al., 2010) were used. To this goal, the wastewater characteristics and the plant
 325 operation conditions such as SRT, HRT, Mixed liquor suspended solid (MLSS) in steady state
 326 condition (g/m³) in the fate model were set to those presented in Suarez et al. 2010. The fate

327 model was run with those parameters at steady state condition. The removal efficiency of the
328 SMX was predicted as -51%, which was somewhat different from that reported by Suarez et al.
329 2010. The removal efficiency was reported based on the parent compound that led to negative
330 removal efficiency. The metabolite compound, which was called daughter compound, during the
331 biotransformation process, was converted to the SMX. The main reason for the difference in
332 removal efficiencies between Suarez et al. 2010 and the calibrated model could be because of the
333 different ratio of the SMX and its metabolite, since in (Suarez et al., 2010) the concentration of
334 metabolite was not reported. This ratio in the calibrated model was inserted from the wastewater
335 characteristics provided by (Plósz et al., 2009). Temperature changes do not have influence on
336 the removal of SMX (Suarez et al., 2010). Removal efficiencies reported in the literature varied
337 in a wide range. For example, eliminations of 33 ± 64 , 0–84% and (-138)–60% can be found in
338 (Castiglioni et al., 2005; GOBEL et al., 2007; Sipma et al., 2010) respectively. The reason for
339 this wide range removal efficiency is due to the fact that real wastewaters, which have a more
340 complex matrix, were used in these works. Negative elimination has also been found in the
341 literature because of presence of conjugated metabolites in the complex wastewater (Plósz et al.,
342 2009; Sipma et al., 2010; Suarez et al., 2010).

343 The submodel for case study 2 was calibrated for both conventional and fate model
344 parameters before running simulations. In the conventional parameter calibration effort,
345 wastewater characteristics, the biomass production at steady state conditions, SRT, and HRT in
346 the system were adjusted to the plant data that were used for the calibration. The batch
347 experimental data presented by (Karahan et al., 2010) was used for the calibration of this model.
348 For the other ASM1 parameters that were not reported in the related literature, the default value
349 for the municipal wastewater treatment plant was inserted into the GPS-X software. The SRT of
350 15 d and HRT of 24 hr were tuned with those of (Karahan et al., 2010). By adjusting the inert
351 organic suspended solids, influent VSS and the ratio of inert particulate COD to biodegradable
352 COD in wastewater influent by trial and error within the GPS-X software and running simulation
353 on the submodel of this case study, the biomass concentration in the bioreactor at steady state
354 was matched with the corresponding experimental data presented in that literature. This relative
355 error for this calibration was 1.6% where the relative error (RE) for the calibration was
356 calculated as $100 * (\text{experimental value} - \text{estimated value for TSS (gXssL-1)}) / \text{experimental value}$
357 for TSS. In the structure of trace compound biodegradation process for recent fate models, the
358 active biomass is not measurable experimentally; thus, it is often assumed that the MLSS or
359 MLVSS can represent the active biomass. In the developed fate model here, the active
360 heterotrophic biomass was used as an active fraction of MLSS and was predicted by the
361 conventional part of the model (Mantis) within the GPS-X. After conventional parameter
362 calibration, according to the plant layout and submodel matrix, the corresponding set of
363 differential equations were transferred to MATLAB where the fate model was calibrated with
364 experimental data reported for the trace compound (NPEO). The calibration for case study 2 is
365 detailed here according to data presented for total COD and NPEO concentration in bulk liquid.
366 The mean μ and standard deviation σ of the literature (Chang et al., 2005; Jahan et al., 2007;
367 Karahan et al., 2010; Zhang et al., 2008) for the parameters of interest were calculated. It should
368 be noted that the values in most references of the literature were reported as uncertainty intervals
369 ($\mu \pm \sigma$), and there was no deterministic range for each parameter reported in the literature. Hence,
370 a total mean and standard deviation over those reported means and standard deviations was
371 calculated. Then lower and upper bounds of each parameter for the calibration were set to $\mu - \sigma$
372 and $\mu + \sigma$, respectively. For this case, the following objective function was considered:

$$SSE = 0.5 \sum_{i=1}^n \left(\frac{Sza_i^{sim} - Sza_i^{exp}}{\max(Sza^{exp})} \right)^2 + 0.5 \sum_{i=1}^n \left(\frac{COD_i^{sim} - COD_i^{exp}}{\max(COD^{exp})} \right)^2 \quad (12)$$

373 where i is the data point index, Sza is the effluent concentration of NPEO in bulk liquid,
 374 the superscripts “sim” and “exp” represent simulation (model) and experimental data from
 375 (Karahan et al., 2010), respectively. Note that the objective function is written in a non-
 376 dimensionalized form to provide relatively similar effects of the two terms on the SSE;
 377 otherwise, the two terms could have such different values that the optimizer would reduce only
 378 the larger term. A summary of the calibration results is presented in the following table:

379

380

Table 4. Calibration results for case study 2

Parameter	Lower Bound	Upper Bound	Optimal Value \pm Standard Error
K_{OCL} (1/d)	0	-	250 \pm 13
K_{hNPEO} (1/d)	0	-	1.45 \pm 0.09
$K_{bioNPEO}$ (m ³ /gbiomass/d)	0.122	0.312	0.237 \pm 0.072

381

382

Table 5. Simulation results of case study 2

Sza_i (g/m ³)	Sza (g/m ³)	Szb (g/m ³)	Szc (g/m ³)	Szd (g/m ³)	SCOD (gCOD/m ³)	xbh (gCOD/m ³)	TSS in AR (g/m ³)	TSS in WAS (g/m ³)
114	0.300	0.570	0.997	35.910	26.530	760.70	1762	3286

383 As mentioned previously, the fate model parameters for NPEOs (case study 2) were
 384 calibrated using data by (Karahan et al., 2010). Following calibration, the fate model simulation
 385 results were validated with data reported by (Zhang et al., 2008). To this goal, the wastewater
 386 characteristics and the plant operation conditions of the fate model were set to those presented in
 387 (Zhang et al., 2008). The value of total COD influent was considered as 232 gCOD/m³ and the
 388 key parameters such as MLSS, SRT, HRT, etc was extracted from (Zhang et al., 2008). The fate
 389 model was run with those parameters at steady state condition. The removal efficiency of the
 390 NPEO was predicted as 98%. Since the SRT was not reported by (Zhang et al., 2008), that value
 391 was set to be 15 days. COD removal efficiency was estimated as 84%.

392 The estimated value was in good agreement with the results reported by (Zhang et al.,
 393 2008), even though the removal efficiency predicted by (Zhang et al., 2008) was 92%, the
 394 calibrated fate model higher estimation removal efficiency could be because of higher SRT than
 395 that of (Zhang et al., 2008). In wastewater treatment, certain design and operational parameters
 396 that affect the fate of micro-constituents can be controlled, while other parameters may be

397 determined by the facility design and/or geographic area. The crucial controllable operational
398 parameter for relatively non-volatile compounds such as XOCs is the solid retention time (SRT),
399 which has been identified in the literature as an important factor (van Bergen et al., 2020; Wang
400 et al., 2020). The importance of this factor in removal of XOCs was investigated via a sensitivity
401 analysis in the GPS-X software.

402 Other parameters in the proposed model, such as biodegradation and sorption rate
403 coefficients (k_b , k_d) have been reported in the literature to span a range of values. Although
404 values for these parameters were computed through a calibration process, to study the robustness
405 of the simulation results, a sensitivity analysis was performed in this work. To this goal, different
406 parameter values were collected from literature; the mean and standard deviation of these were
407 calculated, and separate simulations using $\mu+\sigma$ (upper bound), and $\mu-\sigma$ (lower bound) and the
408 calibrated parameter value for these parameters were run. The results of the various cases were
409 plotted for analysis purposes. For case study 1 the anoxic compartment was excluded to simplify
410 the sensitivity analysis interpretation. SRT has been identified earlier in the literature as an
411 operational parameter that can be used to minimize the effluent concentrations of XOCs (Clara et
412 al., 2005; GOBEL et al., 2007; Kreuzinger et al., 2004; Suarez et al., 2010). The effect of solid
413 retention time on XOC fate over a range of approximately 5 to 20 days at 20°C was investigated
414 in the first case study. The fate model addresses the fate of conventional compounds and
415 xenobiotic organic compounds simultaneously. To explain the effect of SRT on the fate of
416 xenobiotic organic compounds, the effect of SRT on heterotrophic biomass concentration and
417 total suspended solid concentration in the aeration basin were as follows. By setting HRT equal
418 to 10.8hr, the concentrations of active heterotrophic biomass (x_{bh}) and total suspended solids
419 (TSS) in the aeration basin increased as did SRT. Since x_{bh} and TSS in the aeration basin are
420 important parameters in the biodegradation and sorption of SMX, the effect of SRT on the fate of
421 this compound could be explained by the variation of x_{bh} and TSS concentration with respect to
422 SRT. The influent concentration of the soluble (S_{zf}) and particulate (X_{za}) forms of SMX were
423 set at 210 ng/l and 0 ng/l respectively, and the influent concentration of the daughter compound
424 (S_{zg}) was set at 467 ng/l. Figure 5 presents the influence of SRT on the concentration of the
425 soluble form of SMX (S_{zf}) over a range of values of k_d and k_b . Figure 6 presents the
426 corresponding solid phase concentration of SMX (X_{za}) in the waste stream while Figure 7 shows
427 the effluent concentration and rate of biodegradation of S_{zg} . From Figure 5 it can be see that
428 there was a significant reduction in the effluent concentration of S_{zf} (about 34% increase in
429 removal efficiency of S_{zf} between SRT=5 and SRT= 20 days) and S_{zg} (about 15% increase in
430 removal efficiency between SRT=5 and SRT= 20 days). During the biotransformation process,
431 there was an interaction between metabolite compounds (S_{zg}) and the parent compound (S_{zf}).
432 As a result of the biotransformation of S_{zg} , these compounds were converted to the parent
433 compounds and also the parent compound was biodegraded itself. The net result of these
434 biotransformation processes was the production of the parent compound. As can be seen in
435 Figure 5 at SRT= 16 days and k_b and k_d equal to the optimal values, with influent concentration
436 of 210 ng/l, the effluent concentration of S_{zf} was approximately 358 ng/l, so the removal
437 efficiency of S_{zf} was negative. The increase in concentration of active biomass (x_{bh}) due to
438 increase of SRT resulted in increases in the biodegradation rate of S_{zf} (Figure 8) and S_{zg} (Figure
439 7b) (about 27% increase in biodegradation of S_{zf} and 3% increase in biodegradation of S_{zg}).

440 Figure 9 presents the sorption rate for SMX and represents the net effect of the sorption
441 and desorption rates. The positive value shows that the rate of sorption was greater than the rate
442 of desorption. The net sorption rate of SMX increased nearly 32% (Figure 9) over the range of

443 SRTs examined. With the increase of MLSS concentration, the amount of sorbed SMX to the
 444 sludge increases. This is because an increase of suspended solids in the system increases the
 445 number of reactive sites available to absorb SMX from solution. Following that the amount of
 446 SMX sorbed to the sludge was increased. Therefore, the increase of solid sludge in the solution
 447 enhanced the total sorption of SMX (X_{za}) (growth about 88%) by sludge and benefited the
 448 removal of SMX from water phase (Figures 6a and b). However the wastage rate of SMX
 449 decreased with increasing SRT, because for regulating SRT wastage flow rate was increased and
 450 this term was dominant in wastage flow of SMX.

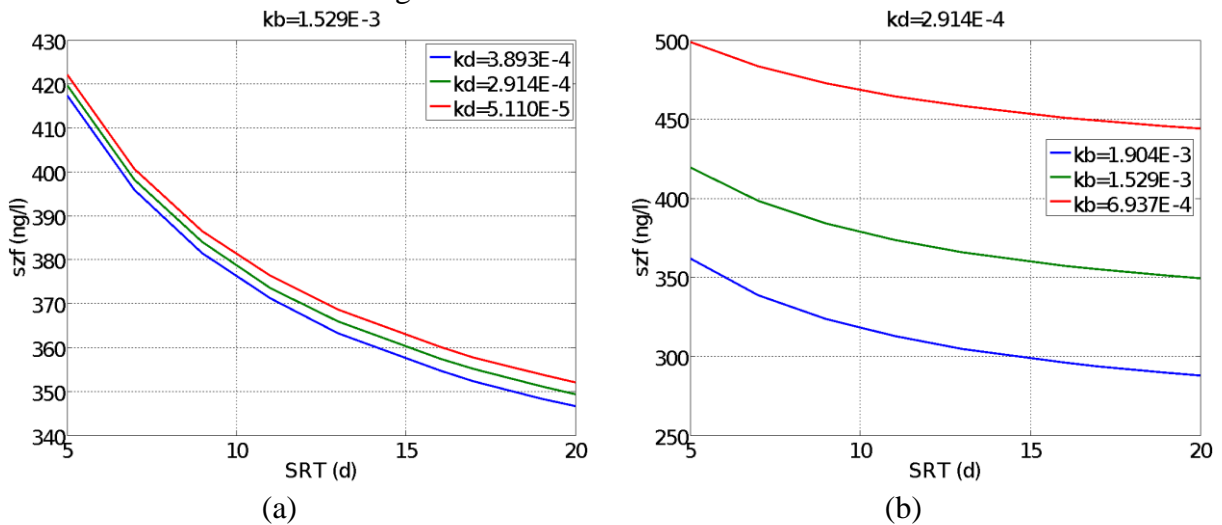


Figure 3. (a) Soluble SMX conc. in the effluent (S_{zf}) with respect to k_d in constant k_b (b) Soluble SMX in effluent (S_{zf}) with respect to k_b in constant k_d , Influent concentration of S_{zf} = 210 ng/l, HRT=10.8hr

451

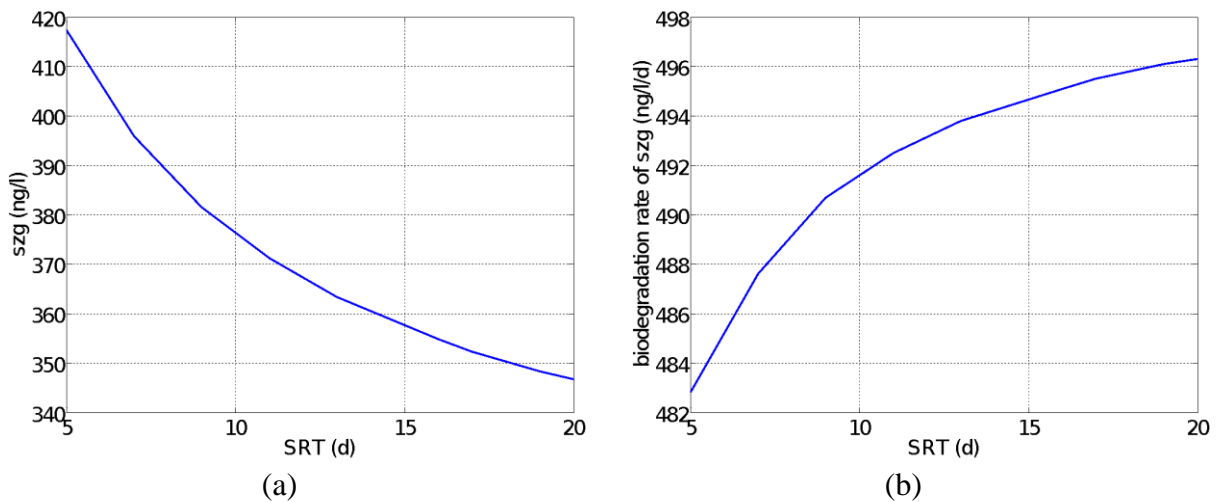


Figure 4. (a) S_{zg} conc. (b) and biodegradation rate for S_{zg} , Influent concentration of S_{zg} = 467 ng/l, HRT=10.8hr

452 To investigate the effect of biodegradation and solid liquid partitioning rate parameters
 453 on the removal of SMX, two different sets of plots (Figures 3,4) have been presented. The first

454 set shows the responses with three different solid liquid partitioning coefficient values ($k_d = \mu + \sigma$,
 455 calibrated value and $\mu - \sigma$) at a fixed biodegradation rate coefficient (set to the calibrated value,
 456 $k_b = 1.529E-3$). The second set demonstrates the effects of varying the biodegradation rate
 457 coefficient ($k_b = \mu + \sigma$, calibrated value and $\mu - \sigma$) at a fixed solid liquid partitioning
 458 coefficient (set to the calibrated value, $k_d = 2.914E-4$). The purpose of presenting these two sets
 459 of plots was to see the influence of these parameters on removal of XOCs.

460 Table 6 shows the percent of SMX removed, biotransformed and wasted at constant k_b ,
 461 SRT= 16 days, and HRT=10.8 hr. Increasing the value of k_d resulted in a decrease of SMX in
 462 the soluble phase and an increase in the concentration of particulate SMX (X_{za}). Therefore, there
 463 was more removal in the liquid and solid phases. Furthermore, at constant k_b , the higher k_d has a
 464 higher net sorption rate, but a lower biodegradation rate, although, there was not a significant
 465 reduction of the biodegradation rate with higher k_d values. The concentration of particulate SMX
 466 (X_{za}) contributed to the wasted mass. Since X_{za} increases in the wastage flow by the sorption
 467 process the wastage percentage was positive, but the removal and biotransformed percentage due
 468 to increasing soluble SMX in effluent were negative.

Table 6. Quantified effects of k_d and k_b on percentage of removed, biotransformed and wasted SMX

Rate Parameter		%removed*	%biotransformed*
$k_b = 1.529E-3$	$K_d1 = 3.893E-4$	-68.95	-78.35
	$K_d2 = 2.914E-4$	-70.19	-77.71
	$K_d3 = 5.110E-5$	-71.47	-77.06
$K_d = 2.914E-4$	$K_b1 = 1.904E-3$	-41	-47.21
	$K_b2 = 1.529E-3$	-70.19	-77.71
	$K_b3 = 6.937E-4$	-114.76	-124.23

* It should be noted that negative %removed and %biotransformed was because of biotransformation of metabolite to the SMX

469 Table 6 also presents the percentage of SMX removed, biotransformed and wasted at
 470 constant k_d with SRT= 16 days, HRT=10.8 hr. With k_d constant, at the higher values of k_b , the
 471 biodegradation rate increases and effluent concentration becomes lower. Therefore, there is more
 472 removal in liquid phase; however, in this case, the sorption rate decreases and the particulate
 473 concentration in solid phase is lower. Generally, at higher SRTs, there was higher removal and
 474 biotransformation of SMX and a lower wasted percentage of SMX (Table 6). The wastage of
 475 SMX decreased with increasing SRT, because the wastage flow rate regulated for SRT control
 476 and this term was dominant in wastage of SMX (See Table 7). The negative removal efficiency
 477 and biotransformation were due to the conversion of the conjugate form to the parent compound
 478 (SMX) that compensated for the biodegradation of SMX. At higher SRT, more of SMX was
 479 biodegraded and at lower SRT, the conversion of the conjugated compound to parent compound
 480 dominated (Table 7).

Table 7. Variation of removed, biotransformed and wasted percentage of SMX at constant k_b and k_d , $k_b = 1.529E-3$, $k_d = 2.914E-4$, versus SRT, HRT=10.8hr

SRT (d)	%removed	%biotransformed	%wasted
5	-99.86	-121.86	22.00

9	-82.86	-94.89	12.03
13	-74.24	-83.03	8.79
16	-70.19	-77.71	7.52
20	-66.38	-72.86	6.48

481 It can be concluded that increases in SRT can enhance removal of SMX and its
 482 metabolite (daughter compound), since at higher SRT, there is higher removal efficiency and
 483 lower waste of SMX and also lower effluent concentration of metabolite. Due to conversion of
 484 metabolite to the parent compound, net biotransformation of the parent compound causes
 485 production of this compound. Therefore, the removal efficiency and also biotransformation rate
 486 of SMX were negative. Furthermore, at SRT higher than 16 days, the removal efficiency does
 487 not change significantly, so SRT=16 days can be reported as the optimal SRT for this case. The
 488 other interesting output of sensitivity analysis states that in the region of low SRT, the
 489 descending rate of effluent concentration of SMX is higher than that of higher region. Finally,
 490 results of Table 6 show the removal efficiency is more sensitive to biodegradation rate than
 491 sorption rate.

492 5 Conclusions

493 In this study, a fate model was developed that can be used to better understand and
 494 optimize the removal of Xenobiotic Organic Compounds (XOCs) in combination with the
 495 removal of traditional pollutants in wastewater treatment plants. Through modeling work, major
 496 mechanisms responsible for removal of XOCs in wastewater treatment were identified and
 497 integrated with an ASM1 model to create an uncalibrated model matrix. Since specific groups of
 498 mechanisms were responsible for the removal of selected compounds, two different case studies
 499 were created for two different groups of compounds. Therefore, two different sub models were
 500 created and categorized within the fate model. Each sub models calibrated and different data sets
 501 were used for the validation process. Sensitivity analysis was carried out against SRT and
 502 biodegradation and sorption coefficients. The major finding of this research can be summarized
 503 as follows: the removal efficiency of the SMX was found to be negative, because the conjugate
 504 was converted to SMX during the biotransformation process. This phenomenon compensates for
 505 biodegradation of SMX. The removal efficiency of XOCs was found to be sensitive to SRT, kb
 506 and kd. Although in most cases the fate model was more sensitive to kb and kd than to
 507 operational. Increases in SRT can enhance removal of all compounds that were studied in this
 508 research. Those compounds include SMX and its conjugate, NPEO. The optimal timeframe can
 509 be reported as 15 days. Sensitivity analysis of three different cases showed that the fate model
 510 was more sensitive to biodegradation rate than to sorption rate.

511 Although the integrated model of this thesis provides a novel framework for XOC fate
 512 simulation, there are still limitations that can be considered for further research on the fate of
 513 XOCs compounds as follows; various reliable sources of experimental data for both XOC and
 514 conventional compounds are important. The availability of this data for both conventional and
 515 trace compounds will lead to more robust and more accurate calibration and validation.
 516 Furthermore, there is a lack of information on XOCs transformation products in the aquatic
 517 systems that can impact the observed fate of the parent compounds in wastewater treatment.
 518 Since a co-metabolism mechanism is involved in the fate of most XOCs, the simultaneous
 519 measurement of primary substrate along with secondary substrate is required to better predict
 520 concentrations of trace organic compounds such as SMX and NPEO.

521

522 **References**

- 523 Achermann, S., Bianco, V., Mansfeldt, C. B., Vogler, B., Kolvenbach, B. A., Corvini, P. F. X., &
524 Fenner, K. (2018). Biotransformation of Sulfonamide Antibiotics in Activated Sludge: The
525 Formation of Pterin-Conjugates Leads to Sustained Risk. *Environmental Science &*
526 *Technology*, 52(11), 6265–6274.
- 527 Adams, C. D. (2008). Modeling the Fate of Pharmaceuticals and Personal Care Products in
528 Sewage Treatment Plants. *Practice Periodical of Hazardous, Toxic, and Radioactive Waste*
529 *Management*, 12(1), 2–9.
- 530 Al Qarni, H., Collier, P., O’Keeffe, J., & Akunna, J. (2016). Investigating the removal of some
531 pharmaceutical compounds in hospital wastewater treatment plants operating in Saudi
532 Arabia. *Environmental Science and Pollution Research*, 23(13), 13003–13014.
- 533 Aymerich, I., Acuña, V., Barceló, D., García, M. J., Petrovic, M., Poch, M., Rodríguez-
534 Mozaz, S., Rodríguez-Roda, I., Sabater, S., von Schiller, D., & Corominas, L. (2016).
535 Attenuation of pharmaceuticals and their transformation products in a wastewater treatment
536 plant and its receiving river ecosystem. *Water Research*, 100, 126–136.
- 537 Baalbaki, Z., Torfs, E., Yargeau, V., & Vanrolleghem, P. A. (2017). Predicting the fate of micro
538 pollutants during wastewater treatment: Calibration and sensitivity analysis. *Science of The*
539 *Total Environment*, 601–602, 874–885.
- 540 Brown, A. K., Ackerman, J., Cicek, N., & Wong, C. S. (2020). In situ kinetics of human
541 pharmaceutical conjugates and the impact of transformation, deconjugation, and sorption on
542 persistence in wastewater batch bioreactors. *Environmental Pollution*, 265, 114852.
- 543 Castiglioni, S., Bagnati, R., Fanelli, R., Pomati, F., Calamari, D., & Zuccato, E. (2005). Removal
544 of Pharmaceuticals in Sewage Treatment Plants in Italy. *Environmental Science &*
545 *Technology*, 40(1), 357–363.
- 546 Çeçen, F., & Gül, G. (2020). Biodegradation of five pharmaceuticals: estimation by predictive
547 models and comparison with activated sludge data. *International Journal of Environmental*
548 *Science and Technology*, 18(2), 327–340.
- 549 Chang, B. V., Chiang, F., & Yuan, S. Y. (2005). Biodegradation of nonylphenol in sewage
550 sludge. *Chemosphere*, 60(11), 1652–1659.
- 551 Cheng, L., Zhang, T., Vo, H., Diaz, D., Quanrud, D., Arnold, R. G., & Sáez, A. E. (2017).
552 Effectiveness of Engineered and Natural Wastewater Treatment Processes for the Removal
553 of Trace Organics in Water Reuse. *Journal of Environmental Engineering*, 143(7),
554 3117004.
- 555 Choudhary, V., & Philip, L. (2021, June). Interpretation of the Risk Associated with Emerging
556 Contaminants in the Aquatic Systems for BRICS Nations. *World Environmental and Water*
557 *Resources Congress 2021*
- 558 Clara, M., Kreuzinger, N., Strenn, B., Gans, O., & Kroiss, H. (2005). The solids retention time a
559 suitable design parameter to evaluate the capacity of wastewater treatment plants to remove
560 micro pollutants. *Water Research*, 39(1), 97–106.
- 561 Compagni, R. D., Polesel, F., von Borries, K. J. F., Zhang, Z., Turolla, A., Antonelli, M., &
562 Vezzaro, L. (2020). Modelling the fate of micro pollutants in integrated urban wastewater
563 systems: Extending the applicability to pharmaceuticals. *Water Research*, 184, 116097.
- 564 Contreras, C. R., López, D., Leiva, A. M., Domínguez, C., Bayona, J. M., & Vidal, G.

- 565 (2019). Removal of Organic Micro pollutants in Wastewater Treated by Activated Sludge
566 and Constructed Wetlands: A Comparative Study. *Water*, 11(12), 2515.
- 567 Draper, N. R. ., & Smith, H. (1981). *Draper, N., and H. Smith: Applied regression analysis*. John
568 Wiley & Sons, New York.
- 569 Gani, K. M., & Kazmi, A. A. (2017). Contamination of Emerging Contaminants in Indian
570 Aquatic Sources: First Overview of the Situation. *Journal of Hazardous, Toxic, and*
571 *Radioactive Waste*, 21(3), 4016026.
- 572 GOBEL, A., MCARDELL, C., JOSS, A., SIEGRIST, H., & GIGER, W. (2007). Fate of
573 sulfonamides, macrolides, and trimethoprim in different wastewater treatment technologies.
574 *Science of The Total Environment*, 372(2–3), 361–371.
- 575 Hai, F. I., Alturki, A., Nguyen, L. N., Price, W. E., & Nghiem, L. D. (2016). Removal of Trace
576 Organic Contaminants by Integrated Membrane Processes for Water Reuse Applications. In
577 *Green Technologies for Sustainable Water Management* (pp. 533–578). American Society
578 of Civil Engineers.
- 579 Hamza, R. A., Iorhemen, O. T., & Tay, J. H. (2016). Occurrence, impacts and removal of
580 emerging substances of concern from wastewater. *Environmental Technology & Innovation*,
581 5, 161–175.
- 582 Hatoum, Potier, Roques-Carmes, Lemaitre, Hamieh, Toufaily, Horn, & Borowska. (2019).
583 Elimination of Micro pollutants in Activated Sludge Reactors with a Special Focus on the
584 Effect of Biomass Concentration. *Water*, 11(11), 2217.
- 585 He, K., Asada, Y., Echigo, S., & Itoh, S. (2018). Biodegradation of pharmaceuticals and personal
586 care products in the sequential combination of activated sludge treatment and soil aquifer
587 treatment. *Environmental Technology*, 41(3), 378–388.
- 588 Jahan, K., Ordóñez, R., Ramachandran, R., Balzer, S., & Stern, M. (2007). Modeling
589 Biodegradation of Nonylphenol. *Water, Air, & Soil Pollution: Focus*, 8(3–4), 395–404.
- 590 Jari, Y., Roche, N., Necibi, M. C., El Hajjaji, S., Dhiba, D., & Chehbouni, A. (2022). Emerging
591 Pollutants in Moroccan Wastewater: Occurrence, Impact, and Removal Technologies.
592 *Journal of Chemistry*, 2022.
- 593 Joss, A., Andersen, H., Ternes, T., Richle, P. R., & Siegrist, H. (2004). Removal of Estrogens in
594 Municipal Wastewater Treatment under Aerobic and Anaerobic Conditions:0.167em
595 Consequences for Plant Optimization. *Environmental Science & Technology*, 38(11), 3047–
596 3055.
- 597 Karahan, Ö., Olmez-Hanci, T., Arslan-Alaton, I., & Orhon, D. (2010). Modelling biodegradation
598 of nonylphenol ethoxylate in acclimated and non-acclimated microbial cultures.
599 *Bioresource Technology*, 101(21), 8058–8066.
- 600 Kreuzinger, N., Clara, M., Strenn, B., & Kroiss, H. (2004). Relevance of the sludge retention
601 time (SRT) as design criteria for wastewater treatment plants for the removal of endocrine
602 disruptors and pharmaceuticals from wastewater. *Water Science and Technology*, 50(5),
603 149–156.
- 604 Lindblom, E., Press-Kristensen, K., Vanrolleghem, P. A., Mikkelsen, P. S., & Henze, M. (2009).
605 Dynamic experiments with high bisphenol-A concentrations modelled with an ASM model
606 extended to include a separate XOC degrading microorganism. *Water Research*, 43(13),
607 3169–3176.
- 608 Maiti, S., Fournier, I., Brar, S. K., Cledon, M., & Surampalli, R. Y. (2016). Nanomaterials in
609 Surface Water and Sediments: Fate and Analytical Challenges. *Journal of Hazardous,*
610 *Toxic, and Radioactive Waste*, 20(1).

- 611 Martin-Pascual, J., López-López, C., Fenice, M., Calero-Díaz, G., Torres, J. C., & Poyatos, J. M.
612 (2020). Effect of Biomass and Operating Condition on Biodegradation Capacity of a Mix of
613 Pharmaceuticals (Carbamazepine, Ibuprofen, and Ciprofloxacin) in a Membrane Bioreactor.
614 *Journal of Environmental Engineering*, 146(6), 4020047.
- 615 Monteoliva-García, A., Martín-Pascual, J., Muñoz, M. M., & Poyatos, J. M. (2019). Removal of
616 a Pharmaceutical Mix from Urban Wastewater Coupling Membrane Bioreactor with
617 Advanced Oxidation Processes. *Journal of Environmental Engineering*, 145(9), 4019055.
618 [https://doi.org/10.1061/\(asce\)ee.1943-7870.0001571](https://doi.org/10.1061/(asce)ee.1943-7870.0001571)
- 619 Nelson, M. I., Alqahtani, R. T., & Hai, F. I. (2018). Mathematical modelling of the removal of
620 organic micropollutants in the activated sludge process: A linear biodegradation model. *The*
621 *ANZIAM Journal*, 60(2), 191-229.
- 622 Park, J., Yamashita, N., Park, C., Shimono, T., Takeuchi, D. M., & Tanaka, H. (2017). Removal
623 characteristics of pharmaceuticals and personal care products: Comparison between
624 membrane bioreactor and various biological treatment processes. *Chemosphere*, 179, 347–
625 358.
- 626 Peng, J., Wang, X., Yin, F., & Xu, G. (2019). Characterizing the removal routes of seven
627 pharmaceuticals in the activated sludge process. *Science of The Total Environment*, 650,
628 2437–2445.
- 629 Plósz, B. G., Leknes, H., & Thomas, K. V. (2009). Impacts of Competitive Inhibition, Parent
630 Compound Formation and Partitioning Behavior on the Removal of Antibiotics in
631 Municipal Wastewater Treatment. *Environmental Science & Technology*, 44(2), 734–742.
- 632 Plósz, B. G., & Ramin, P. (2019). Wastewater-Based Epidemiological Engineering Modeling
633 Illicit Drug Biomarker Fate in Sewer Systems as a Means To Back-Calculate Urban
634 Chemical Consumption Rates. In *ACS Symposium Series* (pp. 99–115). American Chemical
635 Society.
- 636 Pomiès, M., Choubert, J.-M., Wisniewski, C., & Coquery, M. (2013). Modelling of
637 micropollutant removal in biological wastewater treatments: A review. *Science of The Total*
638 *Environment*, 443, 733–748.
- 639 Quintelas, C., Mesquita, D. P., Torres, A. M., Costa, I., & Ferreira, E. C. (2020). Degradation of
640 widespread pharmaceuticals by activated sludge: Kinetic study, toxicity assessment, and
641 comparison with adsorption processes. *Journal of Water Process Engineering*, 33, 101061.
- 642 Rathi, B. S., Kumar, P. S., & Vo, D. V. N. (2021). Critical review on hazardous pollutants in
643 water environment: Occurrence, monitoring, fate, removal technologies and risk
644 assessment. *Science of the Total Environment*, 797, 149134.
- 645 Rodríguez-Escales, P., & Sánchez-Vila, X. (2016). Fate of sulfamethoxazole in groundwater:
646 Conceptualizing and modeling metabolite formation under different redox conditions.
647 *Water Research*, 105, 540–550.
- 648 Sipma, J., Osuna, B., Collado, N., Monclús, H., Ferrero, G., Comas, J., & Rodríguez-Roda, I.
649 (2010). Comparison of removal of pharmaceuticals in MBR and activated sludge systems.
650 *Desalination*, 250(2), 653–659.
- 651 Suárez, S., Lema, J. M., & Omil, F. (2010). Removal of Pharmaceutical and Personal Care
652 Products (PPCPs) under nitrifying and denitrifying conditions. *Water Research*, 44(10),
653 3214–3224.
- 654 van Bergen, T. J. H. M., Rios-Miguel, A. B., Nolte, T. M., Ragas, A. M. J., van Zelm, R.,
655 Graumans, M., Scheepers, P., Jetten, M. S. M., Hendriks, A. J., & Welte, C. U. (2020). *Do*
656 *initial concentration and activated sludge seasonality affect pharmaceutical biodegradation*

657 *rate constants?*

- 658 Wang, Y., Khan, S. J., Fan, L., & Roddick, F. (2020). Application of a QWASI model to produce
659 validated insights into the fate and transport of six emerging contaminants in a wastewater
660 lagoon system. *Science of The Total Environment*, 721, 137676.
- 661 Wang, C., Zhao, J., & Xing, B. (2021). Environmental source, fate, and toxicity of microplastics.
662 *Journal of hazardous materials*, 407, 124357.
- 663 Wilson, M., & Ashraf, M. A. (2018). Study of fate and transport of emergent contaminants at
664 waste water treatment plant. *Environmental Contaminants Reviews (ECR)*, 1(1), 1-12.
- 665 Xiang, Y., Jiang, L., Zhou, Y., Luo, Z., Zhi, D., Yang, J., & Lam, S. S. (2022). Microplastics and
666 environmental pollutants: key interaction and toxicology in aquatic and soil environments.
667 *Journal of Hazardous Materials*, 422, 126843.
- 668 Xue, W., Wu, C., Xiao, K., Huang, X., Zhou, H., Tsuno, H., & Tanaka, H. (2010). Elimination
669 and fate of selected micro-organic pollutants in a full-scale anaerobic/anoxic/aerobic
670 process combined with membrane bioreactor for municipal wastewater reclamation. *Water*
671 *Research*, 44(20), 5999–6010.
- 672 Zhang, J., YANG, M., ZHANG, Y., & CHEN, M. (2008). Biotransformation of nonylphenol
673 ethoxylates during sewage treatment under anaerobic and aerobic conditions. *Journal of*
674 *Environmental Sciences*, 20(2), 135–141.
- 675 Zhou, D., Cai, Y., & Yang, Z. (2022). Key factors controlling transport of micro-and nanoplastic
676 in porous media and its effect on coexisting pollutants. *Environmental Pollution*, 293,
677 118503.
- 678 Zonja, B., Pérez, S., & Barceló, D. (2015). Human Metabolite Lamotrigine-N2-glucuronide Is
679 the Principal Source of Lamotrigine-Derived Compounds in Wastewater Treatment Plants
680 and Surface Water. *Environmental Science & Technology*, 50(1), 154–164.